

# Inversion-asymmetry-induced spin splitting observed in the quantum oscillatory magnetization of a two-dimensional electron system

M. A. Wilde,<sup>1,\*</sup> D. Reuter,<sup>2</sup> Ch. Heyn,<sup>3</sup> A. D. Wieck,<sup>2</sup> and D. Grundler<sup>1</sup>

<sup>1</sup>Physik Department, Lehrstuhl für Physik funktionaler Schichtsysteme, Technische Universität München, James-Frank-Strasse 1, D-85747 Garching b. München, Germany

<sup>2</sup>Ruhr-Universität Bochum, Universitätsstrasse 150, D-44780 Bochum, Germany

<sup>3</sup>Institut für Angewandte Physik, Universität Hamburg, Jungiusstrasse 11, D-20355 Hamburg, Germany

(Received 27 January 2009; published 31 March 2009)

We have investigated the de Haas–van Alphen (dHvA) effect of a two-dimensional electron system in an AlGaAs/GaAs heterojunction which exhibited structure inversion asymmetry. Using torque magnetometry at 30 mK the magnetic quantum oscillations are found to display beating patterns under large tilt angles. We attribute these features to spin splitting of the Fermi surface due to spin-orbit interaction. Such beating patterns in the dHvA effect have been predicted by Bychkov and Rashba more than two decades ago but have not been reported before. From the beat node positions in the magnetization  $M$  we estimate the zero-field spin splitting to be about 200  $\mu\text{eV}$ . Interestingly we find characteristic phase changes in the dHvA signal accompanied by a shift of the discontinuous jump in  $M$  from the high-field to the low-field side of the dHvA oscillations. This observation is unexpected and needs further theoretical explanation.

DOI: 10.1103/PhysRevB.79.125330

PACS number(s): 73.21.Fg, 75.20.-g, 75.40.Cx

## I. INTRODUCTION

Both, the bulk and structure inversion asymmetries (BIA and SIA, respectively) in a III-V semiconductor heterostructure lead to a zero-field spin splitting for a two-dimensional electron system (2DES). The inversion-asymmetry-induced spin-orbit interaction (SOI) is of paramount importance in the field of semiconductor spintronics as, on the one hand, it opens the perspective of controlling spins electrically.<sup>1,2</sup> On the other hand, it is a source of decoherence.<sup>3-5</sup> In 1984, in a pioneering paper, Bychkov and Rashba<sup>6</sup> proposed to measure the magnetic susceptibility and the de Haas–van Alphen (dHvA) effect to observe and quantify the SIA-induced spin splitting in asymmetric heterostructures. The magnetization  $M = -dU/dB$  is a thermodynamic quantity and at low temperature  $T \rightarrow 0$  reflects the variation in the ground-state energy  $U$  with magnetic field  $B$ . In particular, the authors predicted a beating pattern in the quantum oscillatory behavior of  $M$ . Recently transport measurements have allowed to monitor beating patterns in the magnetoresistance  $R(B)$  of 2DES consistent with the Bychkov and Rashba prediction.<sup>7-11</sup>  $R(B)$  monitored at different tilt angles  $\delta$  between the 2DES normal and the direction of  $B$  (cf. Fig. 1) showed a systematic shift of node positions with  $\delta$ . This was explained by the interplay between a SOI-driven zero-field spin splitting and the magnetic-field-induced Zeeman effect.<sup>7</sup> Enlarging  $\delta$  was found to enhance SOI-induced signatures in  $R(B)$  and made them easier to detect.<sup>7,12,13</sup> Corresponding experimental data obtained on  $M(B)$  have not yet been reported. So far, high-resolution dHvA studies have been performed in an almost perpendicular field  $B$ . These experiments were based on either a sophisticated torque magnetometer using torsion balance along a thin wire<sup>14,15</sup> or a specially designed superconducting quantum interference device (SQUID) using very low-noise SQUID electronics at 300 mK.<sup>16,17</sup> These techniques provided a high sensitivity but did not allow to reach high tilt angles  $\delta$ . Only recently

micromechanical torque magnetometers were operated at angles  $\delta$  close to  $90^\circ$ . Here, however, a 2DES in Si/SiGe was explored which did not display a SOI-induced beating pattern.<sup>18</sup>

In this paper we report micromechanical torque magnetometry on a high-mobility 2DES in an AlGaAs/GaAs heterostructure at  $T = 30$  mK. At high tilt angles  $\delta$  we observe beating patterns which we attribute to the inversion-asymmetry-induced spin splitting of the Fermi surface. Beyond the beating pattern we observe characteristic shifts of the dHvA sawtooth shape near a node position. At the same time we find that the spatial orientation of the magnetization  $M$  tilts away from the 2DES normal direction and varies as a

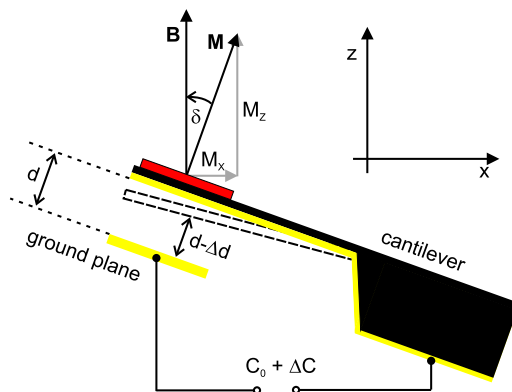


FIG. 1. (Color online) Schematic side view of the experimental setup: micromechanical cantilever prepared from an undoped AlGaAs/GaAs heterostructure (dark color) and mesa containing the high-mobility 2DES (light color). The 2DES normal is tilted by an angle  $\delta$  with respect to the external field  $B$ . A torque  $\tau = \mathbf{M} \times \mathbf{B}$  then acts on the magnetization  $\mathbf{M}$ . The resulting deflection of the 4.5  $\mu\text{m}$  thick cantilever beam is detected by measuring the capacitance  $C_0 + \Delta C$ , where  $C_0$  is the zero-field capacitance and  $\Delta C$  the change induced by  $M$ . At the same time the distance  $d$  between beam and ground plane is changed by  $\Delta d$ .

function of  $B$ . These observations have not been addressed before but will be important if one strives for a quantitative modeling of the SOI-modified dHvA effect in tilted magnetic fields.

The paper is organized as follows. In Sec. II we describe experimental details. In Sec. III we present dHvA measurements in tilted magnetic fields and show that the magnetization exhibits a characteristic beating pattern at high tilt angles. In Sec. III A we employ the model of a parabolic quantum well to analyze the effect of tilted magnetic fields on the magnetization neglecting the effects of SOI. Armed with this knowledge we discuss the beating patterns in detail in Sec. IV. We analyze the data and discuss the results in terms of inversion-asymmetry-induced splitting in Sec. V and conclude with Sec. VI.

## II. EXPERIMENTAL SETUP

We measured the magnetization of a high-mobility 2DES in an AlGaAs/GaAs heterojunction using micromechanical cantilever magnetometry. A schematic sideview of the sensor is shown in Fig. 1. The cantilever sensor was micromachined from undoped AlGaAs/GaAs layers grown by molecular-beam epitaxy following the procedure described in Ref. 19. The 2DES resided in a separate  $10\ \mu\text{m}$  thick mesa which we glued to the end of the flexible beam. The sensor was then mounted on a Swedish rotator immersed in the mixing chamber of a dilution refrigerator. The setup allowed us to adjust the tilt angle  $\delta$  *in situ* at 30 mK. The accuracy was better than  $\pm 0.25^\circ$ . The anisotropic magnetization  $\mathbf{M}$  of the 2DES is measured via the torque  $\boldsymbol{\tau} = \mathbf{M} \times \mathbf{B}$  generated by the external magnetic field  $\mathbf{B}$ . The resulting cantilever deflection is detected using a capacitive readout circuit. The magnetic field  $\mathbf{B}$  is chosen to point in the  $z$  direction, i.e.,  $\mathbf{B} \parallel \mathbf{e}_z$ . In the following the subscripts  $\perp$  and  $\parallel$  mark the components of a vector perpendicular and parallel to the 2DES plane, respectively. The torque acting on  $\mathbf{M}$  at a fixed value of the perpendicular field component  $B_\perp$  increases as  $\tan \delta$ . The sensitivity of the setup thus increases with increasing tilt angle. Note from Fig. 1 that the cantilever magnetometer is directly sensitive to the component  $M_x$  of the magnetization being perpendicular to  $\mathbf{B}$ .

The 2DES was formed in an  $\text{Al}_{0.33}\text{Ga}_{0.67}\text{As}/\text{GaAs}$  heterojunction with a 40 nm spacer separating the 2DES channel from the 72-nm-thick Si-doping layer. All measurements were performed after brief illumination with a red light-emitting diode. Carrier densities  $n_s$  varied from  $3.2 \times 10^{11}$  to  $3.3 \times 10^{11}\ \text{cm}^{-2}$  in different cooling cycles. For a small tilt angle of  $15^\circ$ , we extracted a Landau-level broadening parameter  $\Gamma$  from the dHvA data that was  $\Gamma \leq 0.04\ \text{meV} \times \sqrt{B_\perp [\text{T}]}$ . Following Ref. 20 this value corresponded to a quantum lifetime  $\tau_q = \frac{\hbar}{\Gamma} \geq 1.7 \times 10^{-11}\ \text{s}$  at  $B = 1\ \text{T}$ . The zero-field mobility was  $9 \times 10^6\ \text{cm}^2/\text{V s}$  at 0.3 K measured on a reference sample from the same wafer. The  $M(B)$  data for small tilt angle  $\delta$  were discussed in detail in Ref. 21. There we reported jumps at even integer filling factors  $\nu$  which were discontinuous within the experimental resolution. These jumps substantiated the high quality of the 2DES.

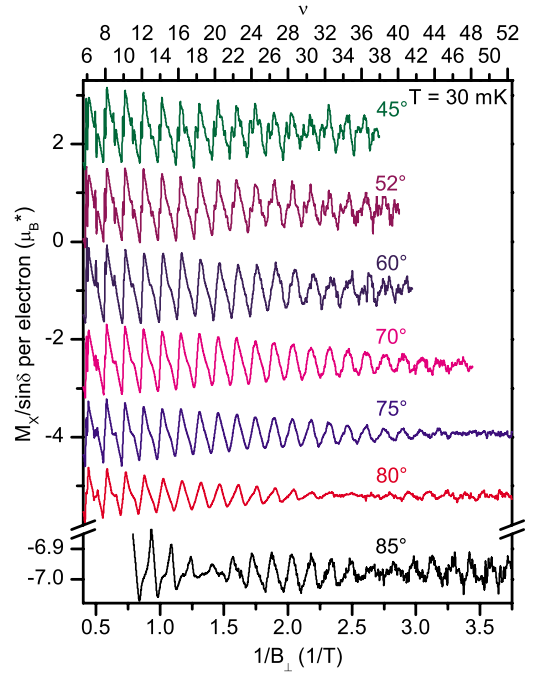


FIG. 2. (Color online) Experimental magnetization  $M$  plotted versus  $1/B_\perp$  for different tilt angles  $\delta$  at  $T = 30\ \text{mK}$ . The data are averaged over both sweep directions to minimize signatures originating from nonequilibrium eddy currents. The curves are offset in vertical direction for clarity. For a fixed filling factor  $\nu$  the dHvA oscillation amplitude decreases with increasing tilt angle for  $\delta > 60^\circ$ . For tilt angles  $\delta \geq 75^\circ$  a beating pattern occurs in the magnetic quantum oscillations.

## III. ANISOTROPIC MAGNETIZATION IN TILTED MAGNETIC FIELDS

In the following we present measurements of the magnetization at  $T = 30\ \text{mK}$  for different tilt angles  $\delta$ . Experimental magnetization data are shown in Fig. 2 versus  $1/B_\perp$ . A smooth background that is due to the magnetic signal of the sensor itself is removed from the raw data by fitting and subtracting a low-order polynomial from the data in  $1/B_\perp$ .<sup>14,22,23</sup> The magnetization exhibits large (small) sawtoothlike oscillations at magnetic field positions where the filling factor  $\nu = n_s / (eB_\perp / h)$  is an even (odd) integer number. In the following we will call these filling factors Landau (spin) filling factors. From the quantum Hall effect it is known that at such field positions the Fermi energy resides in the corresponding energy gaps, i.e., in the Landau quantization or spin-splitting energy gap. We find that at small odd integer filling factor, i.e., at high magnetic field, the dHvA effect is more pronounced than expected from the Zeeman spin-splitting energy for noninteracting electrons. Such an enhancement is known in case of a high-mobility 2DES where electron-electron interaction effects are important.<sup>14,16</sup> SOI is important for spin splitting in particular in small magnetic fields and will be discussed in detail below (Sec. IV).

The magnetization data shown in this paper are averaged over both sweep directions of the magnetic field. Thus magnetic signals from nonequilibrium currents (NECs) induced by the sweeping magnetic field are significantly

diminished.<sup>23</sup> NECs are known to mask the dHvA oscillations.<sup>22,23</sup> In Fig. 2 small residual spikes appear only at low filling factors and low tilt angles due to a slight asymmetry of the NECs for up and down sweep. This leads to an imperfect cancellation. These residual signals are not in the focus of this paper.

To interpret the equilibrium magnetization we assume that the oscillatory part in  $M(B)$  and sawtoothlike signal arise from the perpendicular component  $M_{\perp}$ . The justification for this assumption will be developed in Sec. III A. It allows us to calibrate the oscillation amplitude  $\Delta M$  (peak-to-peak value) in absolute units of  $\mu_B^*$  per electron. At small values of  $\delta$  we find  $\Delta M$  close to  $2\mu_B^*$  for  $\nu \leq 6$ . This value is the maximum amplitude predicted for an ideal 2DES with non-interacting electrons. With increasing tilt angle the in-plane magnetic field  $B_{\parallel}$  increases at fixed  $\nu$ . As can be seen in Fig. 2 the oscillation amplitude  $\Delta M_{\perp}$  decreases strongly and monotonically with increasing  $B_{\parallel}$  for  $\delta > 60^\circ$ . The amplitude at  $\nu=14$  decreases from  $\Delta M_{\perp}=1.45\mu_B^*$  at  $\delta=60^\circ$  to about  $0.7\mu_B^*$  at  $\delta=80^\circ$ . At  $\delta=75^\circ$  the node of a beating enters the oscillation pattern from the low-field side (large filling factors). At  $\delta=80^\circ$  the node position is at about  $\nu=36$ . At  $85^\circ$  it has moved to  $\nu=20$  and a second node at  $\nu=38$  becomes visible. These beating patterns will be analyzed and discussed in terms of SOI in Secs. IV and V. Before, it is important to discuss, both, the spatial orientation of  $\mathbf{M}$  and angular dependence of  $\Delta M$  in the presence of an in-plane field  $B_{\parallel}$ . A modeling thereof has not been developed before.

#### A. DHvA effect of a 2DES with finite thickness in a tilted field

In the following we develop a model for the spatial orientation of  $\mathbf{M}$  of a 2DES and thereby aim for an understanding of the angular dependence of the oscillation amplitude  $\Delta M$  at fixed filling factor  $\nu$ . The understanding will allow us to quantify the oscillatory part  $\Delta M$  of the magnetization signal in *absolute* units and to separate this angular dependence from the observed beating pattern. It turns out that the finite thickness of the 2DES becomes important. It leads to a coupling of electric and magnetic quantizations. At this stage, we neglect spin splitting. The model is valid for arbitrary tilt angles and paves the way for the interpretation of the dHvA effect in tilted magnetic fields following in Sec. IV.

In a magnetic field applied perpendicular to the 2DES plane, the electronic states condense into highly degenerate Landau levels  $E_n=(n+1/2)\hbar\omega_c$ , where  $\hbar\omega_c=\hbar eB_{\perp}/m^*$  is the cyclotron energy ( $m^*$  is the effective mass of the electrons) and  $n=0,1,2,\dots$ . The quantized Landau levels are formed in each subband of the potential well in which the electrons reside. The subband edges have quantized energies  $E_{i,z}$ ,  $i=0,1,\dots$  due to the electric confinement potential. If  $B_{\parallel}$  is zero, the magnetic and electric quantization phenomena are decoupled.<sup>24</sup> Tilting the magnetic field direction away from the surface normal by a tilt angle  $\delta$  leads to a coupling of the electric and magnetic quantizations. The cyclotron frequency  $\omega_c$  and the level degeneracy  $N_L=2eB_{\perp}/h$  depend only on the perpendicular field component  $B_{\perp}=|B|\cos\delta$ . However, the electron eigenenergies become explicitly dependent on  $B_{\perp}$  and  $B_{\parallel}=|B|\sin\delta$  for  $\delta \neq 0$ .

To describe the coupling one needs a model potential for the electronic confinement in growth direction. For the heterojunction of this work one expects a confinement potential of an approximately triangular shape.<sup>24</sup> For such a potential the eigenenergies in tilted fields can be obtained only by perturbation theory.<sup>25</sup> To model the energy spectrum in an analytical way and calculate the magnetization directly for, both, arbitrary tilt angles<sup>26,27</sup> and, in particular, strong in-plane magnetic fields, we follow Ihm *et al.*<sup>28</sup> These authors have assumed a parabolic confinement in the growth direction. Then the confinement effect can be described by a characteristic energy  $\hbar\omega_e$ . To model our sample in growth direction we chose  $\hbar\omega_e \approx (E_{1z}-E_{0z})$ , i.e., we matched the spacing of the first two electronic subbands of the investigated heterostructure. The main outcome of the model, i.e., the qualitative angular dependence of  $\Delta M$ , is found to be insensitive to the exact value of  $\hbar\omega_e$ . Let us for the sake of a convenient notation assume a coordinate frame  $xyz$  with  $\mathbf{e}_z \parallel \mathbf{n}$  and  $\mathbf{e}_x \perp \mathbf{n}$ , where  $\mathbf{n}$  denotes the 2DES surface normal. For a confinement  $V(z)=(m^*/2)\omega_e^2 z^2$  and a tilted magnetic field  $\mathbf{B}=(B_x,0,B_z)$  with the gauge  $\mathbf{A}=(0,B_z x-B_x z,0)$  the Hamiltonian is given by<sup>29</sup>

$$\hat{H} = \frac{\hat{p}_x^2}{2m^*} + \frac{(\hat{p}_y - eB_z x + eB_x z)^2}{2m^*} + \frac{\hat{p}_z^2}{2m^*} + \frac{1}{2}m^*\omega_e^2 z^2. \quad (1)$$

The resulting eigenenergies are

$$E_{i,j} = \hbar\omega_+ \left( i + \frac{1}{2} \right) + \hbar\omega_- \left( j + \frac{1}{2} \right), \quad (2)$$

with the eigenfrequencies

$$2\omega_{\pm}^2 = \omega_c^2 + \Omega^2 \pm \sqrt{(\omega_c^2 - \Omega^2)^2 + 4\omega_{\parallel}^2 \omega_c^2}. \quad (3)$$

Here,  $\omega_{\parallel}=eB_{\parallel}/m^*$  and  $\Omega^2=\omega_c^2+\omega_{\parallel}^2$ . The level structure given by Eqs. (2) and (3) is depicted in Fig. 3(a) for a tilt angle  $\delta=75^\circ$  and confinement potential  $\hbar\omega_e=20$  meV. We find that the in-plane field  $B_{\parallel}$  induces a warping of the Landau levels. The perpendicular and in-plane components of the magnetization vector are calculated by partial differentiation of the systems total energy  $U$  with respect to  $B_{\parallel}$  and  $B_{\perp}$  at  $T=0$  K:

$$M_{\parallel} = - \left. \frac{\partial U}{\partial B_{\parallel}} \right|_N, \quad M_{\perp} = - \left. \frac{\partial U}{\partial B_{\perp}} \right|_N, \quad (4)$$

where  $N$  is the number of electrons.  $U$  is derived by summing over all populated single-particle energies  $E_{i,j}$ . The chemical potential  $\chi$  at  $T=0$  (Fermi energy) is obtained from the condition of constant carrier density  $n_s$ :

$$U = \int_0^{\chi} ED(E)dE \quad \text{and} \quad n_s = \int_0^{\chi} D(E)dE. \quad (5)$$

Using  $D(E)=\sum_{i,j}(2\pi\Gamma)^{-1/2} \exp[-(E-E_{i,j})^2/2\Gamma^2]$  a Gaussian broadening  $\Gamma$  of the Landau levels is considered in the calculations.<sup>30</sup> We took  $\Gamma=0.1$  meV  $\times \sqrt{B[\text{T}]}$ . The calculated components of  $M$  are plotted in Fig. 3(b) for  $\delta=75^\circ$ . It is important to note that only the perpendicular component of  $M$  exhibits the sharp discontinuous jumps characteristic of the dHvA effect. In particular we find that  $M_{\parallel}$  is a continuous

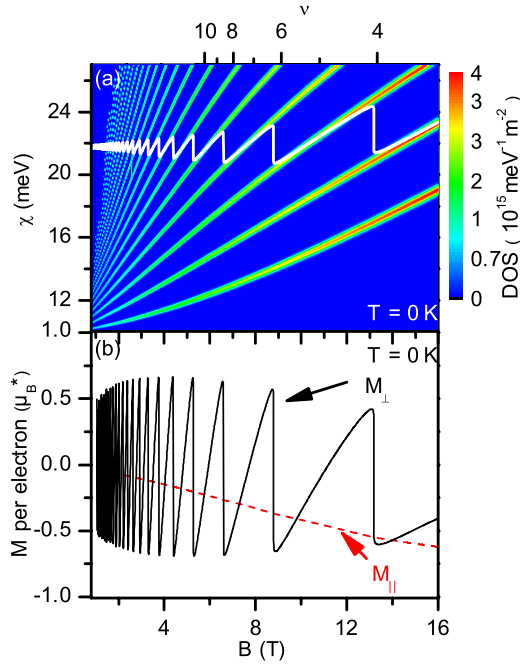


FIG. 3. (Color online) (a) Density of states (DOS) (scale on the right) and chemical potential  $\chi$  (white line). (b) Magnetization components  $M_\perp$  and  $M_\parallel$  for a GaAs 2DES in a tilted magnetic field. The external field is tilted by  $\delta=75^\circ$  with respect to the surface normal. The parameters used here are  $n_s=3.3 \times 10^{11} \text{ cm}^{-2}$  and  $\Gamma=0.1 \text{ meV} \times \sqrt{B[\text{T}]}$ . To solve the problem analytically we assumed a parabolic confinement potential in the growth direction with a level spacing  $\hbar\omega_c=20 \text{ meV}$ .

function of the magnetic field. Even in the limit of  $\Gamma \rightarrow 0$   $M_\parallel$  is continuous at integer filling factors. However, it is no longer continuously differentiable in these positions. This finding also holds for the cases of a rectangular quantum well and a triangular quantum well in growth direction.<sup>31,32</sup> The electrical quantization of the hybrid levels suppresses the Landau fan, i.e., the energetic distance between subband edges is far greater than the Landau-level separation. In other words, only in an ultrastrong magnetic field one would expect a dHvA-type oscillation in the parallel component of  $M$ .

In Fig. 4 we compare  $\Delta M_x$  values extracted from the experiment (cf. Fig. 1) at different  $B_\parallel$  with the model calculation. The qualitative characteristics are in agreement: with increasing  $\delta$  the amplitude  $\Delta M_x$  first increases roughly with  $B_\parallel/B_\perp$  and then decreases again.  $\Delta M_x$  passes thus through a maximum at some given in-plane field  $B_\parallel$ . The decrease in  $\Delta M_x$  is due to the warping of the Landau levels observed in Fig. 3(a) at strong  $B_\parallel$ . Two discrepancies remain: the experimentally observed decrease is stronger than the calculated one and  $\Delta M$  is smaller for  $\nu=14$  than for  $\nu=10$  in the experiment. This is opposite to the model calculations. On the one hand the quantitative discrepancies between experiment and model calculations may be attributed to the assumption of a parabolic quantum well in growth direction. The different systematic dependencies on  $\nu$  could, however, indicate that additional effects occur in the experiment that are not accounted for in our model. On the other hand one may therefore speculate that  $B_\parallel$  leads to a field-dependent increase

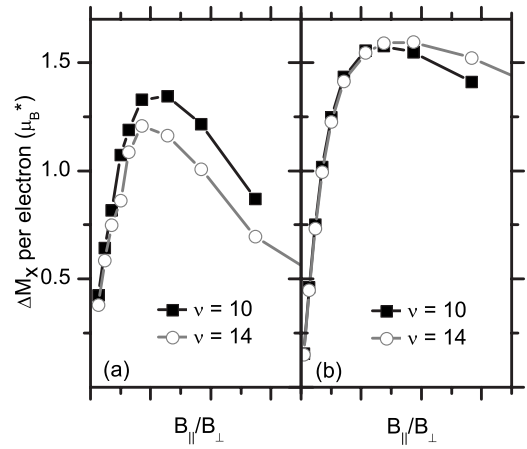


FIG. 4. (a)  $\Delta M_x$  from the experiment and (b) from the parabolic model as a function of  $B_\parallel/B_\perp$ . The overall tilt angle dependence is qualitatively explained by the model.

in the level broadening as suggested in Ref. 7. This arises because the parallel-field-induced Lorentz force pushes 2D electrons toward the heterointerface. As a result scattering by interface roughness or charged centers near the interface is enhanced. Such a mechanism could qualitatively explain our observation because an increased level broadening has a stronger effect on the signal at high filling factors, where the level separation is small.

The model shows that in a field applied under a tilt angle  $\delta$  the magnetization of the 2DES is no longer normal to the 2DES plane.  $M_\perp$  exhibits the discontinuous jumps of the dHvA effect [Fig. 3(b)]. The component  $M_\parallel$  is nonzero and does not show discontinuities as a function of  $B$ . Combining both components the vector  $\mathbf{M}$  varies its spatial orientation depending on the tilt angle  $\delta$  and magnetic field strength.

The important finding is that only  $M_\perp$  exhibits the discontinuous jumps. This allows us to calibrate our data in absolute units: the magnetometer is sensitive to  $M_x$ . In principle we cannot extract the absolute value and direction of  $\mathbf{M}$  from  $M_x$  alone. But since the abrupt jumps of the dHvA effect occur *only* in  $M_\perp$ , the jumps observed in the experimental data  $M$  directly reflect the jumps in  $M_\perp$ . Using this analysis we calculate  $\Delta M_\perp$  in absolute numbers from  $\Delta M_\perp = \Delta M_x / \sin \delta$ . We emphasize that the above model that neglects spin effects does *not* explain a beating pattern in the magnetization.

We are now able to evaluate the magnetization in tilted magnetic fields and will use the findings of this section in our analysis of SOI from  $M$ .

#### IV. BEATING PATTERN IN THE MAGNETIZATION

We now turn to the beating pattern that occurs in the experiment for tilt angles  $\delta \geq 75^\circ$  shown in Fig. 2. In Fig. 5 de Haas–van Alphen measurements performed in a further cool down are shown. The data obtained in different cooling cycles are consistent. In Fig. 5  $M_\perp$  is displayed versus the perpendicular field component  $B_\perp$  for different tilt angles  $\delta$ . At  $\delta=78.5^\circ$  the node of a beating pattern is visible at  $B_\perp \approx 0.4 \text{ T}$  (arrow). With increasing tilt angle the beat node



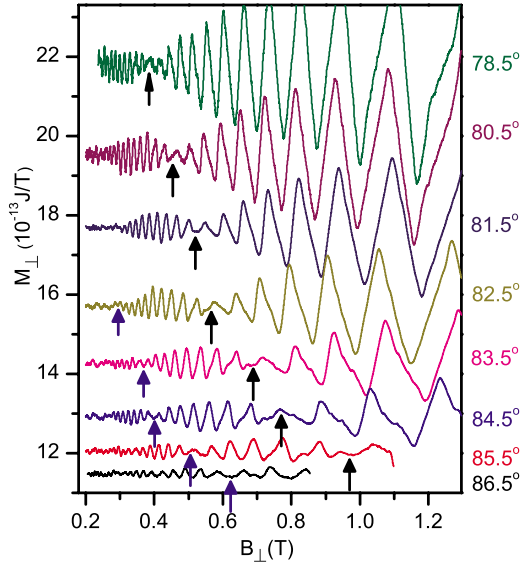


FIG. 5. (Color online) Magnetization  $M$  vs perpendicular magnetic field  $B_{\perp}$  for different tilt angles  $\delta$  at  $T=30$  mK. The curves are offset for clarity. The arrows mark nodes in the beating pattern of the dHvA oscillations. The nodes shift to higher perpendicular field positions with increasing tilt angle.

moves to higher perpendicular fields and at angles  $\delta > 82^\circ$  a second node enters from the left in Fig. 5. Figure 6(a) shows the magnetization for  $\delta=81.5^\circ$  in more detail. Dashed vertical lines mark the positions of integer filling factors as derived from the dHvA effect at high magnetic fields in a perpendicular field. For small  $\nu$ , e.g.,  $\nu=10$ , the almost discontinuous jump in  $M$  is right at the even integer filling factor. The steep flanks of the dHvA signal are on the high-field side of the oscillations as expected for a system with fixed electron number (canonical ensemble). This characteristic shape is expected for all integer filling factors in case of a 2DES with spin-degenerate Landau levels and for a 2DES where only Zeeman splitting lifts the spin degeneracy. We observe in Fig. 6(a) however that for  $28 \leq \nu \leq 36$  the even integer filling factor resides on the flank of *small* slope. We observe a clear  $180^\circ$  phase shift at the beat node near  $\nu=26$ . At this even integer filling factor a local minimum is found in  $M$ . A detailed data analysis between two beating nodes shows that the steep flank moves from the high-field to the low-field side of the dHvA oscillation [Fig. 6(b)]. In the center of the trace where the amplitude  $\Delta M$  exhibits a local maximum the waveform of the dHvA signal is triangular. In other words, the sign change of  $M$  at even integer filling factors depends on the specific magnetic field value. At fixed  $\nu$  the change from paramagnetic to diamagnetic behavior or vice versa varies as a function of tilt angle  $\delta$ . These characteristics have not been discussed before in the literature.

We now analyze the dHvA oscillations employing a fast Fourier transform (FFT) of  $M(1/B_{\perp})$  as shown in Fig. 7. At low tilt angles a single fundamental frequency and its higher harmonics are observed. This confirms that only a single subband is populated by the electrons. At  $\delta=78.5^\circ$  the fundamental frequency peak is split into two distinct frequencies, corresponding to two subsystems of electrons. The

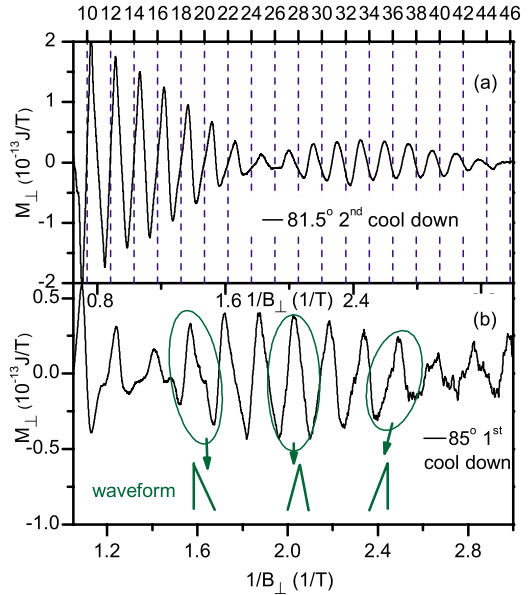


FIG. 6. (Color online) (a) Magnetization vs reciprocal perpendicular magnetic field component for  $\delta=81.5^\circ$ . The dashed vertical lines denote the positions of integer filling factors, i.e., the field positions at which the chemical potential jumps to the next lower lying Landau level. In the orthodox understanding there should be a discontinuous jump at these positions. We observe however a phase shift of  $180^\circ$  at the beat node. (b) Blow up of the low-field data for  $\delta=85^\circ$ . In the center of the depicted trace the waveform of the dHvA signal is triangular. For smaller (larger) values of  $1/B_{\perp}$  the steep flank is on the left (right) of the sawtooth. We observe this behavior reproducibly in all beating patterns at different  $\delta$ .

splitting reflects two different carrier densities in the different subsystems. In the first harmonics the splitting becomes

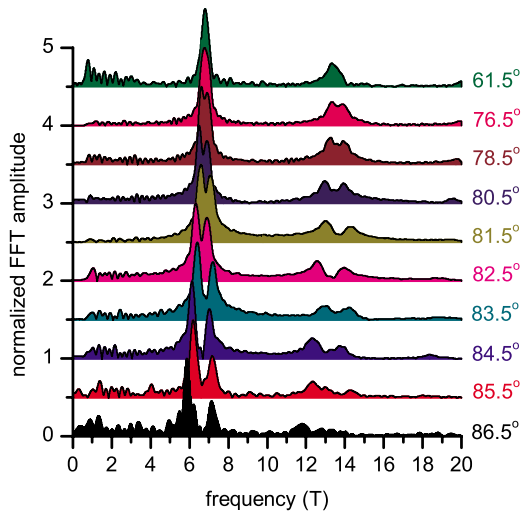


FIG. 7. (Color online) Fast Fourier transforms of dHvA data. For tilt angles below  $75^\circ$  a single fundamental frequency  $f=6.8$  T and its first harmonic are observed, as is exemplarily shown in the topmost curve for  $\delta=61.5^\circ$ . At  $\delta=76.5^\circ$  a shoulder becomes visible in the fundamental frequency peak. A splitting in two distinct maxima is observed at  $\delta \geq 78.5^\circ$ . The splitting increases with increasing tilt angle (cf. Fig. 8).

already visible at  $\delta=76.5^\circ$  and has roughly twice the size of the splitting in the fundamental frequency. The peak corresponding to the sum frequency is weak. In studies relying on magnetotransport investigations in small perpendicular fields  $B$  the relative splitting in  $n_s$  was used to calculate the SOI-induced zero-field spin splitting neglecting the small Zeeman contribution.<sup>8,11</sup> In the presence of a large in-plane field this evaluation, however, is questionable.

## V. ANALYSIS AND DISCUSSION

For the dHvA effect in three-dimensional (3D) systems beating patterns are known to occur whenever different cross-sectional areas of an anisotropic Fermi surface contribute to the signal. In case of a 2DES in GaAs, where the Fermi surface is assumed to be isotropic, the beating suggests that two subsystems of 2D electrons exist. We argue here that these two subsystems arise from the SOI-induced zero-field spin splitting. Since the origin of beating patterns in magnetotransport measurements was controversially discussed in the literature,<sup>33,34</sup> we first address relevant arguments from such a discussion and second evaluate the beating pattern observed in the experiment in Sec. V B.

### A. On the origin of beatings in magneto-oscillations

We address here four relevant arguments concerning the appearance of beating patterns in magneto-oscillations:

(I) Sample inhomogeneities could in principle generate beating patterns. We reported a detailed investigation of the same 2DES in Ref. 21 where we applied  $B$  in the nearly perpendicular orientation. There we showed that  $M(B)$  exhibited an almost perfect sawtooth with negligible smoothing of the oscillations. This behavior reflected a very clean and almost ideal 2DES of high homogeneity.

(II) The mesa containing the 2DES was thinned to a thickness of about 10  $\mu\text{m}$ . It was glued to the flexible beam of the magnetometer. One could assume that the 2DES might be curved or the mesa might contain cracks. If one would consider this the most pronounced beating effect would occur for a sample that was broken into two independent electron systems of equal size being each perfectly flat but tilted with respect to each other. We modeled the magnetization in such a scenario and used the angle between the two systems as a fitting parameter to adjust the position of the last beat node. An angular misalignment of  $\theta=0.32^\circ$  reproduced the positions of the last node for tilt angles  $\delta>76^\circ$ . However, for the second beat node a misalignment of  $\theta=0.40^\circ$  had to be assumed, i.e., the scenario of a static misalignment was not consistent with the experimental data. For two independent electron systems, or—to be more specific—for any other kind of splitting that is field independent the second last node would have to occur at 1/3 of the field of the last node. This is not observed in the experiments. Furthermore, a curvature with  $\theta=0.32^\circ$  of the electron system on the cantilever beam would lead to a smoothing of the magnetization jumps at even  $\nu$ .  $M$  would vary smoothly over a field interval of  $\Delta B > 11$  mT at an tilt angle  $\delta=15^\circ$ . Importantly, we reported abrupt jumps with  $\Delta B < 3$  mT for the same 2DES investi-

gated in the present work.<sup>21</sup> For these reasons we rule out here that a sample consisting of two or more domains with a small angular misalignment is responsible for the observed beating.

(III) For samples with sufficiently high electron concentration  $n_s$  the second electrical subband may be populated. This is obviously not true for tilt angles  $\delta \leq 70^\circ$ , where only one dHvA frequency is observed (cf. FFT spectra in Fig. 7, topmost curve). In addition, in order to produce the beating patterns which we observe, the two subbands must have a very similar electron concentration. This is unlikely for the second subband.

(IV) Magnetointersubband scattering has been reported to produce beating patterns in Shubnikov–de Haas measurements even when the second subband is only thermally populated. We rule out here that in our measurements at  $T = 30$  mK the second subband is thermally populated.

For cases (I, III, and IV) a shifting of the beat node positions with tilt angle is not expected.<sup>34</sup> As a consequence we strongly suggest that the observed beatings patterns reflect the spin-orbit-interaction-induced spin splitting.<sup>7,12,13,35,36</sup> Indeed the tilt angle dependence of node positions has been proposed theoretically in Ref. 36 and used experimentally in Ref. 13 as a tool to identify SOI-induced spin splitting and distinguish it from spurious other effects.

### B. Evaluation of the SOI strength

We now analyze the observed beating patterns in terms of SOI-induced spin splitting. In the frequency (reciprocal magnetic field) domain one can follow the well-established analysis of beatings in Shubnikov–de Haas data.<sup>7,8,10,12</sup> Beat nodes occur when<sup>12,35</sup>

$$\gamma/\hbar\omega_c = (n + 1/2), \quad \text{with } n = 0, 1, 2, \dots, \quad (6)$$

where  $\gamma$  denotes the total splitting. The node positions and the total splitting  $\gamma$  according to Eq. (6) are shown in Figs. 8(a) and 8(b), respectively. The energy splitting in Fig. 8(b) increases strongly with increasing  $B_{\parallel}/B_{\perp}$  and is higher for the second last beat node. This is theoretically predicted.<sup>37</sup> Empirical linear extrapolations to zero parallel magnetic field provide  $\gamma_{n=0}=50$   $\mu\text{eV}$  and  $\gamma_{n=1}=200$   $\mu\text{eV}$  as interceptions. We take these values of  $\gamma$  at  $B=0$  as a first reasonable estimate for input parameters in a more refined modeling below.

In general  $\gamma$  depends on SIA, BIA, and the Zeeman splitting, all of which are coupled (but are not additive) in a tilted magnetic field. Only recently, experimental approaches that separate the SIA and BIA contributions have been developed.<sup>38–40</sup> Giglberger *et al.*<sup>40</sup> measured the relative contributions of Rashba (SIA) and Dresselhaus (BIA) terms in various 2DES in the AlGaAs/GaAs system using spin photocurrents. They found that the Rashba term always dominated over the Dresselhaus term. The highest ratio of the two terms of 7.6 was obtained for a single heterojunction similar to ours, albeit with a 70 nm thick spacer layer and an electron density of  $1.1 \times 10^{11}$   $\text{cm}^{-2}$ . Assuming for the moment that SIA also dominates in our sample we can employ a theoretical description following Refs. 12 and 13 to evaluate our data more quantitatively. In the problem, the Zeeman

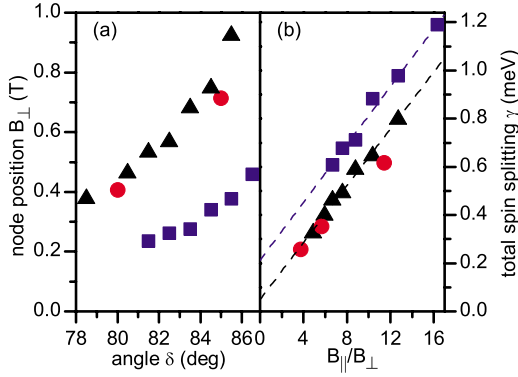


FIG. 8. (Color online) (a) Positions of the beat nodes as a function of tilt angle  $\delta$ . (b) Total splitting vs parallel magnetic field component extracted from (a) using Eq. (6). (■) Splitting at second last node (low-field arrows in Fig. 5). (▲) Splitting at last node (high-field arrows in Fig. 5). (●) Splitting at last node for a different cool down (Fig. 2). The dashed lines are empirical linear fits. The intercepts with the x axis yield estimates of the total splitting at the given node position in perpendicular fields.

term, depending on the total field, couples spin levels of the same Landau level, while the Rashba term couples spin levels belonging to different Landau levels. This leads to a matrix equation that has to be solved numerically.<sup>12</sup> However, as was shown in Ref. 13 recently, a good approximation especially for small splittings can be obtained by considering only the four Landau levels that lie closest to the Fermi level. Thereby, the infinite matrix of the original problem is reduced to a matrix of fourth rank. The resulting quadratic equation can be written as<sup>13</sup>

$$\left(\frac{\gamma}{\hbar\omega_c}\right)^2 = P - 2Q^{1/2}, \quad (7)$$

where

$$P = 2(1 - \beta_z)^2 + 2(\beta_z^2 + \beta_x^2) + (\Delta_R/\hbar\omega_c)^2,$$

$$Q = [(1 - \beta_z)^2 - (\beta_z^2 + \beta_x^2)]^2 + (\Delta_R/\hbar\omega_c)^2(1 + \beta_x^2), \quad (8)$$

with

$$\beta_z = \frac{g\mu_B B_\perp}{2\hbar\omega_c}, \quad \beta_x = \beta_z \tan \delta, \quad (9)$$

and  $\Delta_R$  being the Rashba (SIA) splitting. In this formalism, the dependence of node positions on tilt angle is very sensitive to the value of the  $g$  factor but quite insensitive to  $\Delta_R$ . The broken lines displayed in Fig. 9 match the experimental data at the lowest tilt angle when we take  $g = -0.44$  and  $\Delta_R = 230 \mu\text{eV}$ . As one can see from Fig. 9(b), these values cannot reproduce the large spin-splitting energy  $\gamma$  observed at large tilt angle. The reason might be that either the model is not applicable to our heterojunction, i.e., BIA cannot be neglected, or we have to take into account a different  $g$  factor. Changing  $g$  to  $-1.1$  while assuming  $\Delta_R = 215 \mu\text{eV}$  (solid lines in Fig. 9) leads to high values of  $\gamma$  at large  $B_\parallel/B_\perp$ . However the calculated traces do not remodel the observed functional form. Fitting with a smaller value for the Rashba

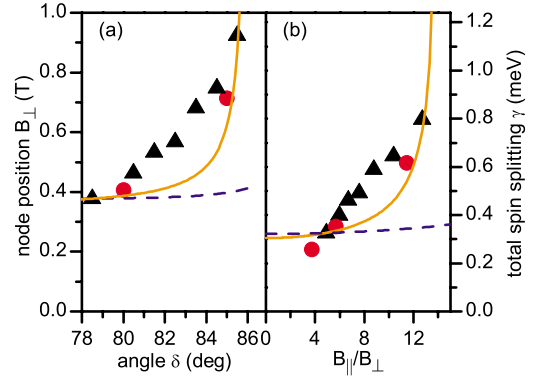


FIG. 9. (Color online) (a) Experimental positions of the last beat node as a function of tilt angle  $\delta$  compared to theoretical predictions [data taken from Fig. 8. (▲) and (●) denote different cool downs]. The dashed line shows the result of the model calculation after Eq. (7) for  $g = -0.44$  and  $\Delta_R = 230 \mu\text{eV}$ . The solid line displays the expected behavior for  $g = -1.1$  and  $\Delta_R = 215 \mu\text{eV}$ . (b) Total splitting vs parallel magnetic field component extracted from (a) using Eq. (6).

splitting leads to large discrepancies concerning the absolute values of the total splitting and the angular positions where node positions should be present in the dHvA effect. Taking  $\Delta_R = 2\alpha k_F$ ,  $k_F = \sqrt{2\pi n_s}$  and a splitting  $\Delta_R = 215 \mu\text{eV}$  yields a Rashba spin-orbit coefficient  $\alpha = 7.5 \times 10^{-13} \text{ eV m}$  for our experimental carrier density. Though there is a discrepancy concerning the functional form for  $\gamma(B_\parallel/B_\perp)$  the evaluated value of  $\alpha$  appears to be reasonable for a 2DES in an AlGaAs/GaAs heterojunction.<sup>10,37,41</sup>

### C. Discussion

In a number of papers, the authors employed models of different levels of sophistication for the interpretation of magnetotransport data reflecting SOI. Authors mostly addressed InAs- or InSb-based heterostructures containing a 2DES. Such III-V semiconductors allowed them to focus on the SIA term since here it was well accepted that the BIA contribution was small. In a GaAs heterostructure the situation is different since opposing results are reported in the literature. Theory has predicted the SIA- and BIA-induced splittings to be of the same order.<sup>42</sup> However, as mentioned above, recent spin photocurrent experiments performed by Giglberger *et al.*<sup>40</sup> suggested that also in a GaAs heterostructure SIA can be much larger than BIA. For tilted field experiments as performed in the present work relevant data are not available. For our analysis carried out in Sec. V B an increased absolute value of  $g$  was necessary to explain large splittings  $\gamma$  in case of a large in-plane field. This suggests an exchange-interaction-enhanced spin splitting which was proposed in Refs. 43–45. Such an interaction effect is already present in dHvA data obtained in a perpendicular magnetic field.<sup>14,30</sup> Assuming an increased value  $|g| = 1.1$  we obtain  $\Delta_R = 215 \mu\text{eV}$ . Theoretical predictions in Ref. 42 would suggest a value between 120 and 140  $\mu\text{eV}$ . Here the authors assumed the BIA contribution to be more important than SIA and stressed that their results depended on the exact value of

the depletion density. This parameter is not known in our experiment. Under these considerations the value extracted from dHvA data seems to be reasonable.

Some of our observations deserve additional discussion:

(i) In the dHvA oscillations, a phase change of  $\pi$  occurs at the beat nodes as shown in Fig. 6(a). This behavior is expected for a beating pattern arising from the interference of two oscillations with slightly different period and can also be seen, e.g., in low-field Shubnikov–de Haas oscillations exhibiting a beating due to SOI. However, in the dHvA data an additional effect is visible: the abrupt jumps in  $M$  can occur on both sides of the sawtoothlike dHvA oscillations depending on filling factor and tilt angle [Fig. 6(b)]. Theoretically, the abrupt jump is expected on the high-field side of the sawtooth for the case of a canonical ensemble, i.e., a system with fixed carrier density and oscillating chemical potential. This case has so far been observed for a 2DES in a semiconductor heterostructure with<sup>20</sup> and without<sup>21</sup> contacts. For a grand canonical ensemble the positions of the jumps are predicted to be on the low-field side.<sup>46–48</sup> Such a scenario has been observed experimentally in Ref. 49: in the organic metal  $\beta''$ -(BEDT-TTF)<sub>2</sub>SF<sub>5</sub>CH<sub>2</sub>CF<sub>2</sub>SO<sub>3</sub> a pair of quasi-one-dimensional (1D) electron surfaces was found to act as a reservoir in addition to the 2D hole pocket that gives rise to the dHvA signal. In our experiment, there is no reason why a field-induced change of the thermodynamic boundary conditions should occur in the system. One may speculate that the observed signal shape might result from competing phase-shifted oscillations which are smoothed out due to the level broadening. The complex behavior of Fig. 6 remains an open question.

(ii) In the FFT of the dHvA data in Fig. 7 two fundamental frequencies and their second harmonics are observed for  $\delta \geq 78.5^\circ$ . The strong second harmonics of the fundamental frequencies are expected due to the sawtooth shape of the oscillatory magnetization. However, the weakness and sometimes absence of the sum frequency peak in Fig. 7 is not understood. A strong sum frequency signature would have been expected for two (spin split) subsystems with a com-

mon Fermi level. A sum frequency signature has been reported for a quantum well where more than one subband was occupied.<sup>50</sup> The FFT resolution is known to depend crucially on the FFT window as well as on the number of oscillations. Still, for well-resolved minima between the harmonics, a complete masking of the sum frequency peak by spectral leakage<sup>51</sup> from the neighboring peaks seems to be unlikely.

The unexpected observations suggest that a full quantum-mechanical treatment of SOI in the presence of SIA, BIA, and Zeeman splitting in tilted magnetic fields would be necessary to remodel quantitatively the dHvA effect in such a complex situation. Since the magnetization is directly related to the ground-state energy of the electronic system, this is an ideal property for direct comparisons between experiment and such a theory. If successfully developed one would take advantage of the entire physical information provided by the magnetization experiment.

## VI. CONCLUSIONS

To summarize, we have observed beating patterns in the magnetization of a 2DES which we attribute to spin-orbit interaction. Such an observation in the dHvA effect was suggested in the pioneering theoretical work by Bychkov and Rashba<sup>6</sup> in 1984. We extract a splitting parameter  $\Delta_R(\alpha)$  of about 215  $\mu\text{eV}$  ( $7.5 \times 10^{-13}$  eV m) from our data in tilted fields. This is slightly larger than theoretical estimates<sup>42</sup> neglecting exchange interaction. The observed characteristic signal shape suggests that the dHvA effect is able to provide complementary information on the inversion-asymmetry-induced spin splitting. For a quantitative remodeling the existing theoretical treatments are not sufficient.

## ACKNOWLEDGMENTS

We thank D. Heitmann for continuous support. Financial support by the Deutsche Forschungsgemeinschaft via the Excellence Cluster “Nanosystems Initiative Munich (NIM)” and the Schwerpunktprogramm 1285 “Halbleiter-Spintronik” via Grant No. GR1640/3 is gratefully acknowledged.

\*mwilde@ph.tum.de

<sup>1</sup>S. Datta and B. Das, *Appl. Phys. Lett.* **56**, 665 (1990).

<sup>2</sup>D. Grundler, *Phys. World* **15**, 39 (2002).

<sup>3</sup>M. I. D’Yakonov and V. I. Perel’, *Sov. Phys. JETP* **33**, 1053 (1971).

<sup>4</sup>R. J. Elliott, *Phys. Rev.* **96**, 266 (1954).

<sup>5</sup>Y. Yafet, *Solid State Physics* (Academic, New York, 1956), Vol. 14.

<sup>6</sup>Y. A. Bychkov and E. I. Rashba, *J. Phys. C* **17**, 6039 (1984).

<sup>7</sup>J. Luo, H. MuneKata, F. F. Fang, and P. J. Stiles, *Phys. Rev. B* **41**, 7685 (1990).

<sup>8</sup>J. Nitta, T. Akazaki, H. Takayanagi, and T. Enoki, *Phys. Rev. Lett.* **78**, 1335 (1997).

<sup>9</sup>G. Engels, J. Lange, T. Schäpers, and H. Lüth, *Phys. Rev. B* **55**, R1958 (1997).

<sup>10</sup>P. Ramvall, B. Kowalski, and P. Omling, *Phys. Rev. B* **55**, 7160

(1997).

<sup>11</sup>D. Grundler, *Phys. Rev. Lett.* **84**, 6074 (2000).

<sup>12</sup>B. Das, S. Datta, and R. Reifengerger, *Phys. Rev. B* **41**, 8278 (1990).

<sup>13</sup>S. A. Studenikin, P. T. Coleridge, G. Yu, and P. J. Poole, *Semicond. Sci. Technol.* **20**, 1103 (2005).

<sup>14</sup>S. A. J. Wieggers, M. Specht, L. P. Lévy, M. Y. Simmons, D. A. Ritchie, A. Cavanna, B. Etienne, G. Martinez, and P. Wyder, *Phys. Rev. Lett.* **79**, 3238 (1997).

<sup>15</sup>M. R. Schaapman, P. C. M. Christianen, J. C. Maan, D. Reuter, and A. D. Wieck, *Appl. Phys. Lett.* **81**, 1041 (2002).

<sup>16</sup>I. Meinel, D. Grundler, S. Bargstaedt-Franke, C. Heyn, D. Heitmann, and B. David, *Appl. Phys. Lett.* **70**, 3305 (1997).

<sup>17</sup>D. Grundler, R. Eckart, B. David, and O. Dössel, *Appl. Phys. Lett.* **62**, 2134 (1993).

<sup>18</sup>M. A. Wilde, M. Rhode, C. Heyn, D. Heitmann, D. Grundler, U.



- Zeitler, F. Schaffler, and R. J. Haug, Phys. Rev. B **72**, 165429 (2005).
- <sup>19</sup>M. P. Schwarz, D. Grundler, I. Meinel, C. Heyn, and D. Heitmann, Appl. Phys. Lett. **76**, 3564 (2000).
- <sup>20</sup>N. Ruhe, J. I. Springborn, C. Heyn, M. A. Wilde, and D. Grundler, Phys. Rev. B **74**, 235326 (2006).
- <sup>21</sup>M. A. Wilde, M. P. Schwarz, C. Heyn, D. Heitmann, D. Grundler, D. Reuter, and A. D. Wieck, Phys. Rev. B **73**, 125325 (2006).
- <sup>22</sup>M. P. Schwarz, M. A. Wilde, S. Groth, D. Grundler, C. Heyn, and D. Heitmann, Phys. Rev. B **65**, 245315 (2002).
- <sup>23</sup>M. Zhu, A. Usher, A. J. Matthews, A. Potts, M. Elliott, W. G. Herrenden-Harker, D. A. Ritchie, and M. Y. Simmons, Phys. Rev. B **67**, 155329 (2003).
- <sup>24</sup>T. Ando, A. B. Fowler, and F. Stern, Rev. Mod. Phys. **54**, 437 (1982).
- <sup>25</sup>A. D. Wieck, F. Thiele, U. Merkt, K. Ploog, G. Weimann, and W. Schlapp, Phys. Rev. B **39**, 3785 (1989).
- <sup>26</sup>J. C. Maan, in *Two Dimensional Systems, Heterostructures, and Superlattices*, edited by G. Bauer, F. Kuchar, and H. Heinrich (Springer-Verlag, Berlin, 1984), p. 183.
- <sup>27</sup>R. Merlin, Solid State Commun. **64**, 99 (1987).
- <sup>28</sup>G. Ihm, M. L. Falk, S. K. Noh, J. I. Lee, and S. J. Lee, Phys. Rev. B **46**, 15530 (1992).
- <sup>29</sup>C. Zhang and Y. Takahashi, Semicond. Sci. Technol. **12**, 835 (1997).
- <sup>30</sup>M. A. Wilde, J. I. Springborn, O. Roesler, N. Ruhe, M. P. Schwarz, D. Heitmann, and D. Grundler, Phys. Status Solidi B **245**, 344 (2008).
- <sup>31</sup>B. Huckestein and R. Kümmel, Phys. Rev. B **38**, 8215 (1988).
- <sup>32</sup>G. Marx and R. Kümmel, J. Phys.: Condens. Matter **3**, 8237 (1991).
- <sup>33</sup>S. Brosig, K. Ensslin, R. J. Warburton, C. Nguyen, B. Brar, M. Thomas, and H. Kroemer, Phys. Rev. B **60**, R13989 (1999).
- <sup>34</sup>A. C. H. Rowe, J. Nehls, R. A. Stradling, and R. S. Ferguson, Phys. Rev. B **63**, 201307(R) (2001).
- <sup>35</sup>B. Das, D. C. Miller, S. Datta, R. Reifenberger, W. P. Hong, P. K. Bhattacharya, J. Singh, and M. Jaffe, Phys. Rev. B **39**, 1411 (1989).
- <sup>36</sup>E. Lipparini, M. Barranco, F. Malet, M. Pi, and L. Serra, Phys. Rev. B **74**, 115303 (2006).
- <sup>37</sup>P. Pfeffer, Phys. Rev. B **55**, R7359 (1997).
- <sup>38</sup>J. B. Miller, D. M. Zumbühl, C. M. Marcus, Y. B. Lyanda-Geller, D. Goldhaber-Gordon, K. Campman, and A. C. Gossard, Phys. Rev. Lett. **90**, 076807 (2003).
- <sup>39</sup>L. Meier, G. Salis, I. Shorubalko, E. Gini, S. Schön, and K. Ensslin, Nat. Phys. **3**, 650 (2007).
- <sup>40</sup>S. Giglberger, L. E. Golub, V. V. Bel'kov, S. N. Danilov, D. Schuh, C. Gerl, F. Rohlfing, J. Stahl, W. Wegscheider, D. Weiss, W. Prettl, and S. D. Ganichev, Phys. Rev. B **75**, 035327 (2007).
- <sup>41</sup>In the present sample measurement of  $g^*$  via the coincidence method based on dHvA data [compare M. A. Wilde, M. Rhode, C. Heyn, D. Heitmann, D. Grundler, U. Zeitler, F. Schaffler, and R. J. Haug, Phys. Rev. B **72**, 165429 (2005)] was not possible. Coincidences should have occurred at an angle  $\delta = \arccos(g^*0.067/2) = 87.9^\circ$  ( $89.2^\circ$ ) for  $|g^*| = 1.1(0.44)$ . At such high angles, i.e., large in-plane fields, the dHvA amplitudes had decreased below the detection limit.
- <sup>42</sup>W. Zawadzki and P. Pfeffer, Semicond. Sci. Technol. **19**, R1 (2004).
- <sup>43</sup>G.-H. Chen and M. E. Raikh, Phys. Rev. B **60**, 4826 (1999).
- <sup>44</sup>C. H. Yang, W. Xu, Z. Zeng, and C. S. Tang, J. Phys.: Condens. Matter **18**, 6201 (2006).
- <sup>45</sup>C. H. Yang and W. Xu, J. Appl. Phys. **103**, 013707 (2008).
- <sup>46</sup>D. Shoenberg, J. Low Temp. Phys. **56**, 417 (1984).
- <sup>47</sup>M. A. Itskovskiy, T. Maniv, and I. D. Vagner, Phys. Rev. B **61**, 14616 (2000).
- <sup>48</sup>T. Champel, Phys. Rev. B **64**, 054407 (2001).
- <sup>49</sup>J. Wosnitza, S. Wanka, J. Hagel, E. Balthes, N. Harrison, J. A. Schlueter, A. M. Kini, U. Geiser, J. Mohtasham, R. W. Winter, and G. L. Gard, Phys. Rev. B **61**, 7383 (2000).
- <sup>50</sup>R. A. Shepherd, M. Elliott, W. G. Herrenden-Harker, M. Zervos, P. R. Morris, M. Beck, and M. Ilegems, Phys. Rev. B **60**, R11277 (1999).
- <sup>51</sup>F. J. Harris, Proc. IEEE **66**, 51 (1978).